Journal of Alloys and Compounds, 206 (1994) 109–112
JALCOM 1007

Correlation between the luminescence and the crystal structure of the hexagonal phase of $RbGd_3F_{10}$

J. Metin[a], R. Mahiou[a,*], C. Linares[b] and M.T. Fournier[a]

[a]*Laboratoire de Chimie des Solides, URA 444 du CNRS, Université Blaise Pascal (Clermont-Fd II), 63177 Aubière Cedex (France)*
[b]*Laboratoire de Physico-Chimie des matériaux Luminescents, URA 442 du CNRS, Université Claude Bernard (Lyon I), 69622 Villeurbanne Cedex (France)*

(Received October 6, 1993)

Abstract

The luminescence of the hexagonal $\beta RbGd_3F_{10}$ is characteristic of the two crystallographically independent sites occupied by the Gd^{3+} ion in this material. The correlation between the spectroscopic and the crystallographic data allows assignment of the $^6P_{7/2}$, $^6P_{5/2} \rightarrow {}^8S_{7/2}$ different emission lines to each site. The luminescence's dynamic is analysed considering two distinct levels in the $^6P_{7/2}$ first excited state.

1. Introduction

The absorption and luminescence spectra of the trivalent lanthanide ions in the solid state present a narrow band structure due to transitions between states of the $4f^n$ configuration. These spectra are characteristic of the structure of the chemical compound as well as the X-ray powder patterns.

The use of Eu^{3+} ion as a structural probe does not always remove the ambiguity concerning the multiplicity of a crystallographic site especially when the narrow $^5D_0 \rightarrow {}^7F_0$ luminescence band is forbidden or when the parameters related to the chemical bond such as geometry, bond angles and lanthanide–ligand distance are very close. In this case, Gd^{3+} ion is especially sensitive [1]. The ground state of the $4f^7$ configuration of the Gd^{3+} ion is $^8S_{7/2}$, which is only slightly split by the crystal field; therefore it is possible to deduce information concerning the multiplicity of the regular sites from the number of the Stark components of the $^6P_J \rightarrow {}^8S_{7/2}$ transitions. We report here the results of our investigation on the luminescence of the hexagonal phase $\beta RbGd_3F_{10}$ and discuss them in relation to the structural data.

2. Experimental details

All the luminescence measurements were performed on polycrystalline samples. The compounds are synthesized in the solid state by reacting stoichiometric mixtures of the starting fluorides: RbF (Merck: 99.98%, dehydrated at 500 °C under a secondary vacuum), YF_3 and GdF_3 (prepared from Y_2O_3 and Gd_2O_3, Rhône Poulenc: 99.9%).

The reaction mixtures carried out in a glove box, are finely ground, introduced in sealed nickel tubes and heated at 850 °C for 48 h. The experimental device used for the optical measurements has been previously described [2] (resolutions: emission 0.02 nm; excitation 0.005 nm).

3. Structural background

$\beta RbGd_3F_{10}$ (high temperature form), isostructural with KYb_3F_{10} [3] crystallizes in the hexagonal system, with the space group $P6_3mc$. In this structure, the eight-coordinated trivalent ion occupies two crystallographic sites 6c (point symmetry C_s). Calculation of the Gd–F distances for each rare earth coordination polyhedron gives the values listed in Table 1 (average distance

TABLE 1. Different Y–F distances in $\beta RbGd_3F_{10}$

Gd(1)-F distances (Å)			Gd(2)-F distances (Å)		
Gd(1)–F(1)	2.18	(×2)	Gd(2)–F(4)	2.25	(×2)
Gd(1)–F(2)	2.24	(×2)	Gd(2)–F(1)	2.33	(×2)
Gd(1)–F(7)	2.39		Gd(2)–F(5)	2.39	
Gd(1)–F(6)	2.41		Gd(2)–F(3)	2.41	
Gd(1)–F(3)	2.41	(×2)	Gd(2)–F(7)	2.41	(×2)
Average distance	2.31		Average distance	2.35	

*Author to whom correspondence should be addressed.

SSDI 0925-8388(93)01007-T

Gd(1)–F: 2.31 Å and average distance Gd(2)–F: 2.35 Å).

3. Results

3.1. Luminescence emission and crystal field analysis

The spectra shown in Figs. 1 and 2 were recorded at 300 K upon excitation at 314.3 nm ($^8S_{7/2} \rightarrow {}^6P_{7/2}$ transition). The emission lines correspond to the radiative relaxation from the $^6P_{7/2}$ and $^6P_{5/2}$ Stark levels to the $^8S_{7/2}$ ground state. We found eight separate lines for the $^6P_{7/2} \rightarrow {}^8S_{7/2}$ transition and six lines for the $^6P_{5/2} \rightarrow {}^8S_{7/2}$ transition. The line profiles are independent of the wavelength and of the power of the excitation beam. These results indicate the existence of Gd^{3+} ions in $\beta RbGd_3F_{10}$ at two sites with the same coordination and point symmetry.

In Figs. 1 and 2, the peaks related to the two Gd^{3+} sites are respectively labelled A_i and $B_i (i = 1\text{–}7)$. This differentiation was based on the relative intensity between the A and B emission lines. The position of the recorded emission lines are listed in Table 2.

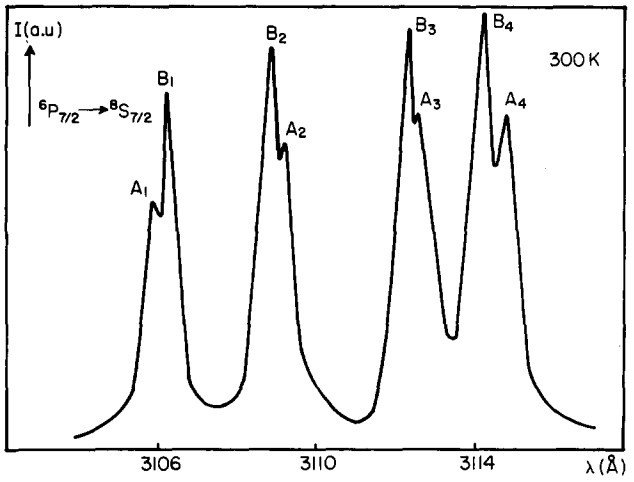

Fig. 1. $^6P_{7/2} \rightarrow {}^8S_{7/2}$ emission spectrum of $\beta RbGd_3F_{10}$ at 300 K.

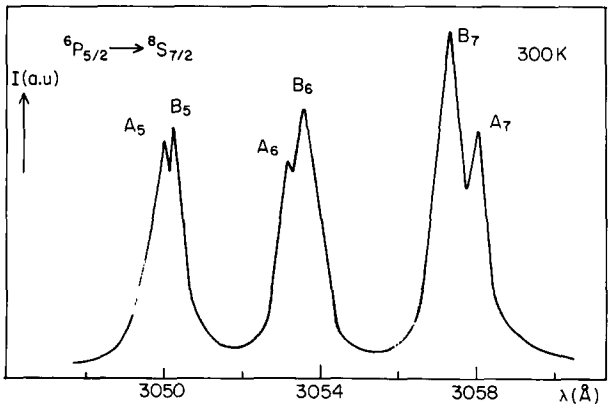

Fig. 2. $^6P_{5/2} \rightarrow {}^8S_{7/2}$ emission spectrum of $\beta RbGd_3F_{10}$ at 300 K.

A comparison between the observed and calculated positions obtained by crystal field analysis (Table 2) was made. The splittings of the ^6P_J levels ($J = 7/2$, 5/2, 3/2) for Gd^{3+} depend exclusively on the second order crystal field parameters [4, 5]. The three independent sets of B_0^2 and B_2^2 are given according to the Wybourne notation [6].

The average quadratic error for the seven ^6P_J levels for both A and B sites are, respectively the following:

10.1 cm^{-1} and 8.3 cm^{-1} for the first set;

9.9 cm^{-1} and 8.1 cm^{-1} for the second set;

9.9 cm^{-1} and 8.1 cm^{-1} for the third set.

These errors do not allow us to select one of the three parameter series.

3.2. Relation with the crystal structure

It is well known that the splittings decrease as the distance to the ligand increases [7]. Therefore, when looking at the Gd–F average distance, it is possible to assign the A_i emission lines to the Gd(1) ion and the B_i emission line to the Gd(2) ion. It is worth mentioning the very weak difference between the barycentres of the levels relative to the A and B sites (< 5 cm^{-1} for the ^6P_J terms). This information implies that the nephelauxetic shifts for the two sites are equivalent. Thus, the Gd–F distances in each of the two sites are very close, in agreement with the crystallographic data.

3.3. Luminescence decays and dynamical processes

Upon excitation in one of the Stark components of the $^6P_{7/2}$ multiplets we have analysed the $^6P_{7/2} \rightarrow {}^8S_{7/2}$ luminescence decays of Gd^{3+} ion at different temperatures.

At 300 K, the decay shows purely exponential behaviour with a time constant of 675 μs. This value lies largely below the $^6P_{7/2}$ lifetime i.e. 6.5 ms measured in the weakly doped $\beta RbGd_{0.5}Y_{2.5}F_{10}$ compound. It shows an energy diffusion among the Gd^{3+} ions and a transfer to impurities. When the temperature is decreased down to the temperature range 40–150 K the $^6P_{7/2} \rightarrow {}^8S_{7/2}$ luminescence decay of Gd^{3+} ions is no more exponential but two time constants can be obtained; a fast one τ_f and a slow one τ_s. The component τ_f is affected by a decreasing temperature whereas the component τ_S has a value similar to the time constant measured at room temperature. In Fig. 3 we have plotted the $^6P_{7/2} \rightarrow {}^8S_{7/2}$ luminescence decay at 300 K and 50 K. At 50 K, τ_f and τ_S keep, respectively, the values 210 μs and 620 μs.

In the fast diffusion model where the decay time is purely exponential, the lifetime fits the following expression:

TABLE 2. Crystal field parameters, observed and calculated positions and assignments of the $^6P_J \rightarrow {}^8S_{7/2}$ emission lines of Gd^{3+} in $\beta RbGd_3F_{10}$

	Nominal state	Label	Experimental energies (cm^{-1}) (wavelengths in nm)	Barycentre (cm^{-1})	Calculated energies (cm^{-1})		
					Set 1	Set 2	Set 3
Site A	$^6P_{7/2}$	A_4	32105.8 (311.47)		32092.8	32093.3	32003.7
		A_3	32127.5 (311.26)		32132.9	32131.3	32131.1
		A_2	32162.6 (310.92)	32148.2	32165.4	32165.1	32164.2
		A_1	32196.8 (310.59)		32201.7	32203.1	32203.8
		A_7	32701.1 (305.80)		32719.0	32718.8	32718.8
		A_6	32752.5 (302.32)	32747.2	32747.5	32747.2	32747.2
		A_5	32788.0 (304.99)		32775.1	32775.6	32775.6
Crystal field parameters (cm^{-1})					$B_0^2=460$ $B_2^2=\pm180$	$B_0^2=0$ $B_2^2=\pm375$	$B_0^2=-460$ $B_2^2=\pm180$
Average quadratic error (cm^{-1})					10.1	9.9	9.9
Site B	$^6P_{7/2}$	B_4	32109.9 (311.43)		32099.0	32099.2	32100.0
		B_3	32130.6 (311.23)		32135.5	32134.3	32134.5
		B_2	32166.8 (310.88)	32149.9	32165.5	32165.7	32164.5
		B_1	32192.6 (310.63)		32200.0	32200.8	32201.0
	$^6P_{5/2}$	B_7	32708.6 (505.76)		32721.3	32721.0	32721.3
		B_6	32748.2 (305.36)	32747.2	32747.2	32747.2	32747.2
		B_5	32784.7 (305.02)		32773.1	32773.4	32773.1
Crystal field parameters (cm^{-1})					$B_0^2=420$ $B_2^2=\pm170$	$B_0^2=0$ $B_2^2=\pm350$	$B_0^2=-420$ $B_2^2=\pm170$
Average quadratic error (cm^{-1})					8.3	8.1	8.1

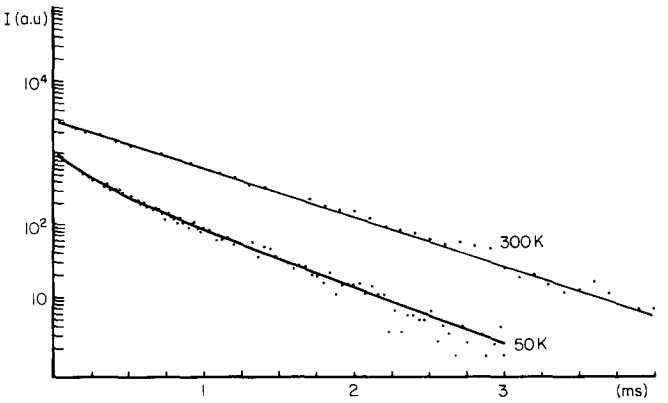

Fig. 3. Luminescence decays of the $^6P_{7/2} \rightarrow {}^8S_{7/2}$ emission of Gd^{3+} in $\beta RbGd_3F_{10}$ at 300 K and 50 K: ... experimental data —— (50 K) fitting according to eqn. (2).

$$\tau^{-1} = \tau_0^{-1} + 4\pi D C_A f$$

where τ_0^{-1} is the radiative decay without transfer, C_A and f are, respectively, the concentration and the radius of sphere of influence of the acceptor ions (here impurities) and D is the effective diffusion coefficient. A chemical analysis has allowed us to estimate a maximum concentration of impurities (essentially Tb^{3+} and Eu^{3+}) of 5.4×10^{19} ions cm^{-3} while the Gd^{3+} total concentration is 1.08×10^{22} ions cm^{-3}.

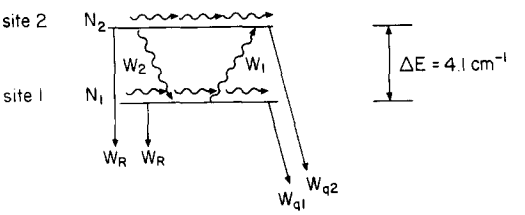

Fig. 4. Schematic representation of the two levels system: W_R^{-1} = radiative decay rate; W_2 = direct transfer rate between the two sites; W_1 = back transfer rate between the two sites; $W_1 = W_2 \exp(-\Delta E/k_B T)$; W_Q = transfer rate to impurities.

With $\tau = 675$ μs, $\tau_0 = 6.5$ ms and $f = 4.16$ Å (weighted average distance between nearest and next-nearest neighbours assuming a short-range ion–ion interaction), we obtain a diffusion coefficient $D = 5\times10^{-11}$ cm^2 s^{-1} at 300 K.

For the lower temperatures, as mentioned above, the luminescence decay is non-exponential. The same shape is observed whatever wavelength is chosen in the lowest energy emission band (~311.5 nm). We have tried to fit the time dependence of the luminescence intensity with the expressions of the Heber's [8] or Yokata and Tanimoto's [9] models in the case of a limited diffusion process.

None of the expressions reproduces correctly the luminescence decay profiles. So we have used a model

with two levels in the excited state (Fig. 4) characteristic of both Gd^{3+} ions in each site. In the case of fast diffusion, the population rate equations can be written as:

$$N_1 = -(W_R + W_1 + W_{Q1})N_1 + W_2 N_2$$
$$N_2 = -(W_R + W_2 + W_{Q2})N_2 + W_1 N_1 \quad (1)$$

where 1 and 2 correspond to each of the two sites occupied by the Gd^{3+} ion. N_i is the population of the $^6P_{7/2}$ level of Gd^{3+} in site i ($i=1,2$), W_R is the radiative decay rate, and W_{Qi} is the transfer to impurities or defects. W_1 and W_2 are the transfer rates between the 1 and 2 levels. In view of the small energy gap between the 1 and 2 levels (lower than 5 cm^{-1}) for $T>40$ K, we take $W_1 = W_2 = W (W_1 = W_2 \exp(-\Delta E/K_B T)$. Moreover the recorded luminescence decay contains simultaneously the deexcitation from levels 1 and 2. With $N(t) = N_1(t) + N_2(t)$, the population $N(t)$ is given by

$$N(t) = A \exp(-t/\tau_f) + B \exp(-t/\tau_S) \quad (2)$$

where $\tau_f^{-1} = (W_{Q1} + W_{Q2} + 2W_R + 4W)/2$

$$\tau_S^{-1} = (W_{Q1} + W_{Q2} + 2W_R)/2$$

Equations (1) were solved assuming that $|W_{Q1} - W_{Q2}| \ll 2W$, ($W_{Q1} \sim W_{Q2}$), because the two Gd^{3+} sites are equivalent, and the range of experimental temperature is relatively high.

In Fig. 3 where we have plotted the $^6P_{7/2} \rightarrow {}^8S_{7/2}$ luminescence decay recorded at 50K, the drawn line shows the good agreement obtained using eqn. (2). The derived τ_f and τ_S take the values 210 μs and 620 μs as mentioned above. This leads us to a transfer rate W between the two Gd^{3+} sites, which is about 1575 s^{-1} at 50 K. As the value of W_R is known to be 154 s^{-1}, we can estimate the total transfer probability W_Q to the impurities

$$W_Q = W_{Q1} + W_{Q2} = 2917 \ s^{-1}$$

4. Discussion

We have pointed out optically the two crystallographic sites for Gd^{3+} in $\beta RbGd_3F_{10}$ using luminescence spectra as well as dynamics. Small variations of bond angles and distances are clearly evidenced by the emission spectra where the line shapes indicate that the Gd^{3+} ions present in the structure are divided into two independent sites. Moreover as the temperature is decreasing below 150 K, the non-exponentiality of the luminescence decays strongly suggests a cross-over from a fast diffusion regime to a diffusion-limited regime. The model used to describe the luminescence decays (sum of two exponentials) has not allowed us to observe this cross-over. This indicates that the mechanism of energy transfer from each of the two Gd^{3+} sites is different.

In conclusion, analysis of the luminescence properties of the hexagonal phase $\beta RbGd_3F_{10}$ confirms the structural description of this compound in which two independent crystallographic sites for the rare earth have been assumed. Consequently, the Gd^{3+} ion is a structural site probe which is especially sensitive to coordination polyhedra.

References

1 A. Aamili, R. Mahiou, C. Linares, D. Zambon, D. Avignant and J.C. Cousseins, *J. Solid State Chem., 95* (1991) 307 and references cited therein.
2 R. Mahiou, J. Metin, M.T. Fournier, J.C. Cousseins and B. Jacquier, *J. Lumin., 43* (1989) 51.
3 S. Aleonard, J.C. Guittel, Y. le Fur and M.T. Roux, *Acta Crystallogr., B32* (1976) 3227.
4 E. Antic-Fidancev, M. Lemaitre-Blaise and P. Caro, *J. Chem. Phys., 76* (1982) 2906.
5 H.D. Jones and B.R. Judd, *Phys. Rev. B, 2* (1970) 2319.
6 B.G. Wybourne, *Spectroscopic Properties of Rare Earths,* Interscience, New York, 1965.
7 P. Caro, E. Antic, L. Bearing, O. Beaury, J. Derouet, M. Faucher, C. Guttel, O.K. Moune and P. Porcher, *Colloque International du CNRS, Lyon (1976),* Editions du CNRS, Paris, 1977, p. 71.
8 J. Heber, *Phys. Stat. Solidi, (b) 48* (1971) 319.
9 M. Yokota and O. Tanimoto, *J. Phys. Soc., Jpn, 22* (1967) 779.